Schild's Ladder for the parallel transport of deformations in time series of images

Lorenzi Marco[1,2], Nicholas Ayache[1], Xavier Pennec[1], and the Alzheimer's Disease Neuroimaging Initiative *

[1] Project Team Asclepios, INRIA Sophia Antipolis, France
[2] LENITEM, IRCCS San Giovanni di Dio, Fatebenefratelli, Italy

Abstract. Follow-up imaging studies require the evaluation of the anatomical changes over time for specific clinical groups. The longitudinal changes for a specific subject can be evaluated through the non-rigid registration of successive anatomical images. However, to perform a longitudinal group-wise analysis, the subject-specific longitudinal trajectories of anatomical points need to be transported in a common reference frame. In this work, we propose the Schild's Ladder framework as an effective method to transport longitudinal deformations in time series of images in a common space using diffeomorphic registration. We illustrate the computational advantages and demonstrate the numerical accuracy of this very simple method by comparing with standard methods of transport on simulated images with progressing brain atrophy. Finally, its application to the clinical problem of the measurement of the longitudinal progression in the Alzheimer's disease suggests that an important gain in sensitivity could be expected on group-wise comparisons.

1 Introduction

One of the main objectives in the field of computational anatomy concerns the modeling of the dynamics occurring in specific clinical groups. This is motivated by the need to generalize the characteristics observed in the single patients, by performing group-wise statistics. The aim of the Template-based analysis is therefore to describe the subject-specific characteristics in a normalized reference by transporting the individual geometries in a common space. Different normalization methods can be used for static observations, depending on the complexity of the feature of interest: resampling for scalar values, reorientation for vectors, and more advanced methods for tensors, like Preservation of the Principal Directions (PPD) or the Finite Strain (FS) [1].

* Data used in preparation of this article were obtained from the Alzheimer's Disease Neuroimaging Initiative (ADNI) database (www.loni.ucla.edu/ADNI). As such, the investigators within the ADNI contributed to the design and implementation of ADNI and/or provided data but did not participate in analysis or writing of this report. A complete listing of ADNI investigators can be found at:www.loni.ucla.edu/ADNI/Collaboration/ADNI_Authorship_list.pdf

Transport of longitudinal trajectories The problem of modeling dynamic quantities, such as the changes measured in time series of images, is a more complex issue. This problem concerns the consistent transport of the trajectories of changes in a common reference, and we are interested in the behaviour of the transported dynamics, especially regarding the ability to preserve the original amount of expansion/contraction in homologous regions.
A key issue is the different nature of the changes occurring at the intra-subject level, which reflects the biological phenomena of interest, and the changes across different subjects. In fact, the inter-subject variability is a scale of magnitude higher than the more subtle subject-specific variations.
Different approaches for the transport have been proposed depending on the type of measure of change that is considered (time series of jacobian images, the time-varying initial momentum, displacement fields as a function of time, etc.). A simple method of transport consists in *reorienting* the longitudinal inter-subject displacement *vector field* by the Jacobian matrix of the subject-to-template mapping. A drawback of this method is that the longitudinal deformation is fully combined to the inter-subject one. The method proposed by [10] uses the *transformation conjugation* (change of coordinate system) from the group theory in order to compose the longitudinal inter-subject deformation with the subject-to-template one. As pointed in [3], this practice could potentially introduce variations in the transported deformation and relies on the inverse consistency of the estimated deformations, which can raise problems for large deformations. The *parallel transport* of relational measures was introduced in [12] in the context of the Large Deformation Diffeomorphic Metric Mapping (LDDMM) [8]. The notion of parallel transport proposed here consists in translating a vector *along a geodesic* while preserving the parallelism according to the space geometry. This framework allows to transport the geodesic diffeomorphic registration for both point supported data and images, and it was applied to study the hippocampal shape changes in Alzheimer's disease [9]. Although it represents a rigorous implementation of the parallel transport, it is limited to the transport along geodesics and it comes to the price of a computationally intense scheme. This is a limitation which could prevent the application to large datasets with multiple time series of images, which are now becoming more easily available to the imaging community.
In tensor based morphometry, the transport is used to normalize in a common reference frame the degree of changes in specific regions, such as the hippocampal volume loss in the brain. For this purpose, it is also possible to directly normalize the measures of change by interpolating the Jacobian determinant scalar map of the intra-subject longitudinal change into the template reference [3]. However, the Jacobian determinant represents only one of the several features of interest in morphometric studies (like full jacobian matrices, tensors or the flux [4], [7]). Moreover, transporting the original deformation trajectory allows multivariate group analysis like evaluation of mean deformations, PCA, etc.

The aim of the present paper is to propose an accurate computational approach for the parallel transport of longitudinal trajectories of images, and con-

sequently of vectors and related measures of changes. For this purpose we introduce in Section 2 the "Schild's Ladder", which proves to provide a fast and well posed diffeomorphic solution for the transport of longitudinal trajectories of images along any curve. To demonstrate the effectiveness of the scheme, we then apply it in Section 3 to the specific clinical problem of the measurements of the longitudinal progression of atrophy in Alzheimer's disease.

2 The Schild's Ladder Procedure

The Schild's Ladder was introduced in the last century in the field of the general relativity by the physicist Alfred Schild [5]. It provides a straighforward method to compute a first order approximation of the parallel transport of a vector along a curve without requiring the knowledge of the tangent structure of the space.

Let M a manifold and C a curve parametrized by the parameter τ with $\frac{\partial C}{\partial \tau}|_{T_0} = \mathbf{u}$, and $\mathbf{A} \in T_{P_0}M$, a tangent vector on the curve at the point $P_0 = C(0)$. Let P_1 be a point on the curve relatively close to P_0, i.e. separated by a sufficiently small parameter value τ.

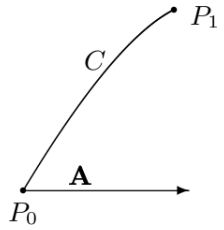

The Schild's Ladder computes the parallel transport of $\mathbf{A}$ along C:

1. Define a *curve* on the manifold parametrized by a parameter σ passing through the point P_0 with tangent vector $\frac{\partial}{\partial \sigma}|_{P_0} = \mathbf{A}$. Chose a point P_2 on the curve separated by P_0 by the value of the parameters σ. The values of the parameters σ and τ should be chosen in order to construct the Schild's Ladder within a single coordinate neighborhood.
2. Let l be the *geodesic* connecting $P_2 = l(0)$ and $P_1 = l(\lambda)$, we chose the "middle point" $P_3 = l(\lambda/2)$. Now, let us define the *geodesic* r connecting the starting point P_0 and P_3 parametrized by ρ such that $P_3 = r(\rho)$. Extending the geodesic at the parameter 2ρ we reach the point P_4. We can now pick a *curve* connecting P_1 and P_4. The vector A' tangent to the curve at the point $P1$ is the parallel translation of A along C.
3. If the distance between the points P_0 and P_1 is large, the above construction can be iterated for a sufficient number of small steps.

The Schild's ladder geometrical approximation resides in the assumption that all the geometrical information of the space are encoded by the geodesics. Although the geodesics on the manifold are not sufficient to recover all the information about the space properties, such as the connection, it has been shown that the Schild's Ladder describes the parallel transport with respect to the symmetric part of the connection of the space [6]. An intuitive proof is that the

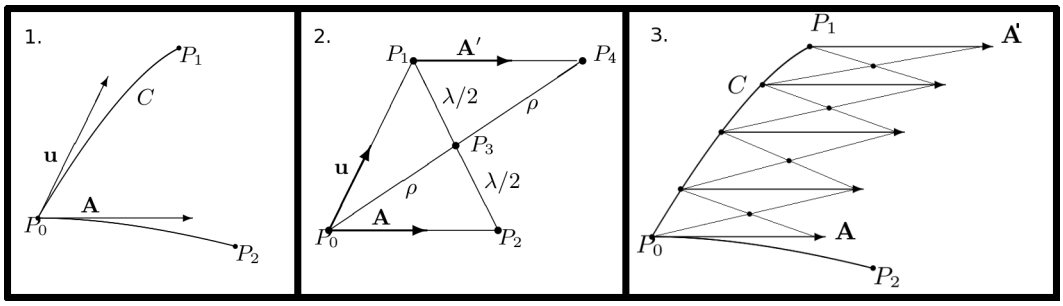

construction of the above diagram is commutative and can be symmetrized with respect to the points P_1 and P_2. If the original connection is symmetric, then this procedure provides a correct linear approximation of the parallel transport of vectors.

2.1 Application to Images

Schild's Ladder for images Let I_i $(i = 1 \dots n)$ be a time series of images with the baseline I_0 as reference. Consider a template image T_0, the aim of the procedure will be to compute the image T_i in order to define the transport of the sequence $I_0 - I_i$ in the reference of T_0. In the sequel, we focus on the transport of a single image I_1.

To apply the Schild's Ladder in the context of the images, we define the paths in the space of images by action from the space of diffeomorphism. Let $\mathbb{I} = \{f : \mathbb{R}^3 \to \mathbb{R}\}$ the image space and let us define the action $* : M \times \mathbb{I} \to \mathbb{I}$ given by $(\varphi, I) \mapsto \varphi * I = I \circ \varphi^{-1}$, where M is the space of the diffeomorphisms. If the distance between two images in the image space is defined in terms of diffeomorphisms [12], then the geodesics in the image space are defined by the action of the geodesic paths in the space of the diffeomorphisms.

The Schild's Ladder procedure can therefore be naturally translated in the following way:

1. The geodesic $l(\lambda)$ in the space $\mathbb{I}$ connecting I_1 and T_0 is such that $l(0) = g(0) * I_1 = I_1$ and $l(1) = g(1) * I_1 = T_0$.
2. Define the half-space image $I_{\frac{1}{2}}$ as $l(1/2) = g(1/2) * I_1$.
3. Compute the geodesic $r(\rho) = h(\rho) * I_0$ connecting I_0 and $I_{\frac{1}{2}}$ such that $r(0) = I_0$ and $r(1) = h(1) * I_0 = I_{\frac{1}{2}}$.
4. Define the transported follow-up image as $T_1 = r(2) = h(2) * I_0$.

Finally one can evaluate the transported deformation, and the related measures of changes, in the new reference by registering the images T_0 and T_1.
Despite its straightforward formulation, the application of the Schild's Ladder

to the image space requires multiple evaluations of geodesics in the space of diffeomorphisms and a consequent high cost in terms of computation time and resources. Moreover, it assumes an exact matching, which is bound to lead to important numerical problems. For instance, the definition of $I_{\frac{1}{2}}$ using the forward deformation on I_1 or the backward from T_0 lead to very different results. We propose to reformulate the above scheme in a computationally efficient and numerically stable framework using only transformations.

An effective Schild's Ladder using one parameter subgroups. We use the setting of the stationary velocity fields (SVF) diffeomorphic registration as provided by the Symmetric Log Demons algorithm [11]. In particular we base the Schild's Ladder construction on the path defined by the Lie group exponential of vectors.We note that the SVF is a valid approximation of a small step of a time-varying velocity field diffeomorphism. Given a pairs of images I_i, $i \in \{0, 1\}$, the SVF framework parametrizes the diffeomorphism φ required to match the reference I_0 to the moving image I_1 by a stationary velocity field u. The velocity field u is an element of the Lie Algebra $\mathbf{G}$ of the Lie group of diffeomorphisms M, i.e. an element of the tangent space at the identity $T_{id}M$. The diffeomorphism φ belongs to the one parameter subgroup generated by u and is parametrized by the Lie group exponential operator $\varphi = \mathrm{Exp}(u)$. We can therefore define the paths in the space of the diffeomorphisms from the one parameter subgroup parametrization $l(\lambda) = \mathrm{Exp}(\lambda \cdot u)$ and by consequence the paths in the image space by the action *.

However, the Schilds Ladder in the image space requires a number of interpolations and exponentiations, which could introduce biases due to the numerical approximations. Moreover the registration is constrained to be smooth and it is therefore impossible to reach a perfect match of corresponding intensities in the registered images. We however take advantage of the symmetry of the construction in order to be robust to the changes introduced by the registration and lead to a very simple scheme.

1. Let $I_1 = \mathrm{Exp}(u) * I_0$.
2. Compute $v = argmin_{v \in \mathbb{G}} \left(\|T_0 \circ \mathrm{Exp}(-v/2) - I_1 \circ \mathrm{Exp}(v/2)\|^2 + \|v^2\| \right)$. The half space image $I_{\frac{1}{2}}$ can be defined in terms of $v/2$ as $\mathrm{Exp}(-v/2) * T_0$ or $\mathrm{Exp}(v/2) * I_1$. While from the theoretical point of view the two images are identical, the choice of one of them, or even their mean, introduces a bias in the construction. The definition of the half step image can be bypassed by relying on the symmetric construction of the parallelogram (Figure 1).
3. The transformation from I_0 to $I_{\frac{1}{2}}$ is $\rho = \mathrm{Exp}(v/2) \circ \mathrm{Exp}(u)$ and the symmetry leads to

$$\mathrm{Exp}\left(\Pi(u)\right) = \rho \circ \mathrm{Exp}(-v/2) = \mathrm{Exp}(v/2) \circ \mathrm{Exp}(u) \circ \mathrm{Exp}(-v/2)$$

The transport of the deformation $\varphi = \mathrm{Exp}(u)$ can be therefore obtained through the conjugate action operated by the deformation parametrized by $v/2$. In opposition to the standard conjugate method which operates "vertically",

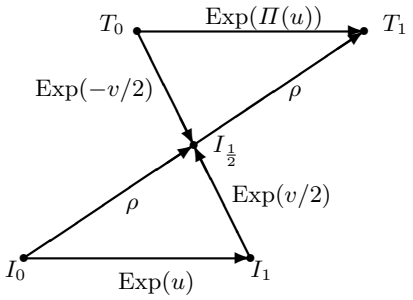

Fig. 1: Schild's Ladder parallelogram with the one parameter subgroups. The transport $\mathrm{Exp}(\Pi(u))$ is the deformation $\mathrm{Exp}(v/2) \circ \mathrm{Exp}(u) \circ \mathrm{Exp}(-v/2)$

from the image I_0 to T_0, here the transport operates "diagonally".
Since the direct computation of the conjugate by composition is potentially biased by the discrete approximation, we propose two different schemes to correctly evaluate the transport directly in the Lie Algebra.

BCH formula for the conjugate action The Baker Campbell Haudorff (BCH) formula was introduced in the SVF diffeomorphic registration in [2] and provides an explicit way to compose diffeomorphisms by operating in the associated Lie Algebra. More specifically, if v, u are static velocity fields, then $\mathrm{Exp}(v) \circ \mathrm{Exp}(u) = \mathrm{Exp}(w)$ with $w = v + u + \frac{1}{2}[v,u] + \frac{1}{12}[v,[v,u]] - \frac{1}{12}[u,[u,v]] + \ldots$. In particular, for small u, the computation can be truncated to any order to obtain a valid approximation for the composition of diffeomorphisms. For example, the use of a truncated expansion $v + u + \frac{1}{2}[v,u]$ is used as updating rule for the Symmetric Log Demons algorithm. Applying the truncate BCH to the conjugate action leads to

$$\Pi_{BCH}(u) \simeq u + [v,u] + \frac{1}{2}[v,[v,u]]$$

To provide a sufficiently small vector for the computation of the conjugate we can take advantage of the properties of the one-parameter subgroups to observe that

$$\begin{aligned} &\mathrm{Exp}(v) \circ \mathrm{Exp}(u) \circ \mathrm{Exp}(-v) = \\ &= \mathrm{Exp}(\frac{v}{n}) \circ \ldots \circ \mathrm{Exp}(\frac{v}{n}) \circ \mathrm{Exp}(u) \circ \mathrm{Exp}(-\frac{v}{n}) \circ \ldots \circ \mathrm{Exp}(-\frac{v}{n}) \end{aligned}$$

The conjugation can then be iteratively computed in the following way:

- find n such that v/n is small.
- compute $w = u + [\frac{v}{n}, u] + \frac{1}{2}[\frac{v}{n}, [\frac{v}{n}, u]]$

– Let $u = w$
– Iterate the above construction (n steps).

Using the BCH formula allows to perform the transport directly in the Lie algebra and avoids exponentiation and the interpolations, thus reducing the bias introduced by the numerical approximations. Moreover, this methods preserves the original "Ladder" formulation, operated along the path described by $\mathrm{Exp}(tv)$. However, it requires a number of iterations to be computed.

Conjugate action from the exponential map We can provide an alternative and direct formula to compute the transport by conjugate action from the definition of the exponential:

$$\mathrm{Exp}(u) = \lim_{n\to\infty} \left(\mathrm{Id} + \frac{u}{n}\right)^n.$$

We can then write:

$$\mathrm{Exp}(\Pi_{conj}(u)) = \lim_{n\to\infty} \left(\mathrm{Exp}(v) \circ \left(\mathrm{Id} + \frac{u}{n}\right) \circ \mathrm{Exp}(-v)\right)^n$$

Let $y = \mathrm{Exp}(-v)(x)$ and $\phi(x) = \mathrm{Exp}(v)(x)$, then

$$\begin{aligned}\mathrm{Exp}(\Pi_{conj}(u)) &= \lim_{n\to\infty} \left(\phi\left(y + \frac{u(y)}{n}\right)\right)^n = \\ &= \lim_{n\to\infty} \left(\mathrm{Id} + \frac{1}{n}\left(\mathrm{D}(\phi(y))|_{\phi^{-1}(x)} \cdot u \circ \phi^{-1}(x) + o(\|u\|^2)\right)\right)^n\end{aligned}$$

By the definition of the exponential map, we obtain then a first order approximation for the transported vector given by

$$\Pi_{conj}(u) = \mathrm{D}\left(\mathrm{Exp}(v)\right)|_{\mathrm{Exp}(-v)} \cdot u \circ \mathrm{Exp}(-v)$$

We note that $\mathrm{D}\left(\mathrm{Exp}(v)\right)|_{\mathrm{Exp}(-v)} = \mathrm{D}\left(\mathrm{Exp}(-v)\right)^{-1}$. This method provides a closed form formula which enables to compute the transport by reorienting the field $u \circ \mathrm{Exp}(-v)$ by the matrix field $\mathrm{D}\left(\mathrm{Exp}(v)\right)$ resampled by $\mathrm{Exp}(-v)$, or equivalently, by the matrix field $\mathrm{D}\left(\mathrm{Exp}(-v)\right)^{-1}$. The second formula requires however the inversion of a matrix which is an operation potentially unstable. In the following, the transport $\Pi_{conj}(u)$ will be evaluated through the resampling by linear interpolation of the matrix $\mathrm{D}\left(\mathrm{Exp}(v)\right)$.

From a theoretical point of view the results obtained from the two methods are equivalent in the continuous domain

$$\Pi_{conj}(u) = u + Dv \cdot u - Du \cdot v + O(\|v\|^2) \simeq \Pi_{BCH}(u)$$

3 Experiments on synthetic and real data

3.1 Comparison of different methods of transport

We created the realistic simulated deformations based on the deformation field that matches the baseline scan (I_0) of a patient from the ADNI dataset to the 1-year follow-up of the same patient, computed using the Symmetric Log-Demons Algorithm. The ventricular expansion was extracted by masking the corresponding SVF v for a mask including the ventricles. The deformations in the remaining areas of the brain were imposed to be negligible, by setting the velocity field to 0 and adding gaussian noise. The SVF v was then increasingly scaled ($v_i = f_i v$, with $f_i = 0.5, 1, 2, 3$) and the resulting deformations fields $\varphi_i = \text{Exp}(v_i)$ were used to warp the baseline scan I_0 to generate a longitudinal progression of serial images I_i with increasing ventricular expansions.

The longitudinal progression was then transported in a new reference given by the image of another patient (target space T_0) along the deformation ψ_T using different methods:

- Schild's Ladder (Π_{BCH} and Π_{conj}),
- conjugate method: $Ad_{\psi_T}(\varphi_i) = \psi_T^{-1} \circ \varphi_i \circ \psi_T$
- interpolation of the scalar maps by the mapping ψ_T,
- reorientation of the static velocity field v_i by the Jacobian Matrix of the deformation ψ_T: $J_{\psi_T} v_i$.

As summarized in Table 1, not all the methods operate on the same features and a direct comparison is not always possible. To test the accuracy of the transport, the differents methods were quantitatively compared on the scalar measures representing the amount of change induced in the ventricles mask. The analyzed features were: Jacobian determinant of the transported deformation $J = \det\nabla\varphi_i$, Log-Jacobian determinant of the transported deformation $log(J)$, Elastic Energy $\|v_i\|^2_{El} = tr\left((\text{Id} + \nabla\varphi_i)(\text{Id} + \nabla\varphi_i)^T\right)$, and L^2 norm of the SVF $\|v_i\|_{L^2}$.

	SVF (u)	Transformation ($\varphi = \text{Exp}(u)$)	Scalar Measure (J,log J, $\|u\|$, $\|u\|_{El}$)
Interpolation of Scalar	No	No	Yes
Conjugate action	No	Yes	Yes
Schild's Ladder	Yes	Yes	Yes
Reorientation	Yes	Yes	Yes

Table 1: Different methods of transport and transported features. From the SVF we can infer transformations from which we can extract scalar measures, while the reverse is not possible.

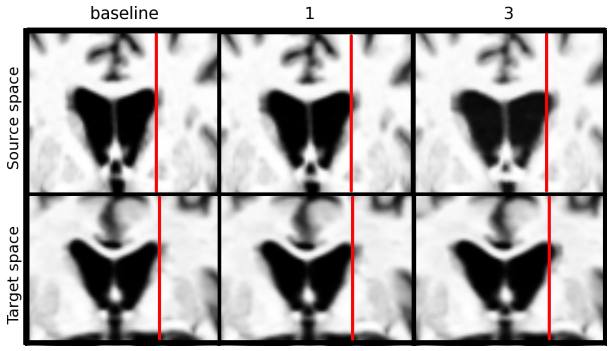

Fig. 2: Transport of time series of images. Top row: original longitudinal trajectory for the ventricular expansion at the different scaling factors. Bottom row: transported longitudinal sequence in the target space.

Results The synthetic time series of images transported by the Schild's Ladder can be appreciated in Figure 2. The series is consistent with the original trajectory of ventricular expansion while adapting to the new reference. Concerning the quantitative comparison of the different transport methods, Figure 3 shows the Log-Jacobian scalar image derived from the different methods. As expected, either the Conjugate method and the Reorientation lead to noisy maps. We can see that for both the Schild's Ladder (BCH scheme) and the Interpolation method, the resulting Jacobian map seems to adapt to the new reference space while remaining sufficiently smooth, coherently with the original map. The map resulting from the conjugate scheme of the Schild's Ladder (not shown) was more noisy than the BCH one.

Table 2 shows the amount of changes measured with the different methods. For all of them, the longitudinal trend was in agreement with the original one. The methods performed differently depending on the measure of interest, but we can note that the Schild's Ladder provides, in most of the cases, the closest measure to the one in the original reference. Moreover, the BCH version of the Schild's Ladder performs on the average better as compared to the conjugate one.

3.2 One year follow-up changes on Alzheimer's disease

Images corresponding to the baseline I_0 and the one-year follow-up I_1 scans were selected for 70 subjects affected by Alzheimer's disease from the Alzheimer's Disease Neuroimaging Initiative (ADNI) database (www.loni.ucla.edu/ADNI). For each subject i, the pairs of scans were bias corrected and symmetrically rigidly aligned by iterative registration to the mean intensity image. The baseline was linearly registered to the MNI standardized template and the parameters of

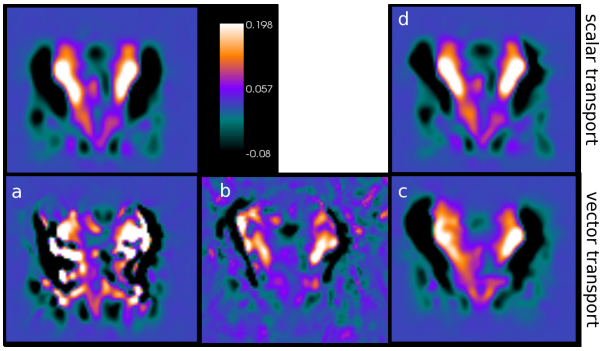

Fig. 3: Log-Jacobian maps of the transported deformation field in the target space T. Top left: Log-Jacobian map corresponding to the intra-subject deformation $\varphi_1 : I_0 \rightarrow I_1$ in the baseline space. From a) to d), Log-Jacobian maps in the target space T corresponding to the transported deformation with the different methods: a) Reorientation, b) Conjugate, c) Schild's Ladder (BCH version), d) Interpolation of the scalar Log-Jacobian original image.

the transformation were applied to I_1^i. Finally, for each subject, the longitudinal changes were measured by non-rigid registration using the Symmetric Log Demons algorithm with regularization parameters $\sigma_{elastic} = 2$ and $\sigma_{fluid} = 1$. The resulting deformation fields $\varphi_i = \text{Exp}(v_i)$ were transported in a common reference by using the Schild's Ladder (BCH scheme). The group-wise longitudinal progression was modeled as the median of the transported stationary velocity fields. Finally, the areas of significant longitudinal expansion/contraction were investigated by one-sample t-test on the group of Log-Jacobian maps corresponding to the transported deformations, with the multiple comparisons controlled by a statistical threshold of $p < 0.01$ corrected for false discovery rate (FDR).

	L^2 norm				Elastic energy				Jacobian (avg-1)				Log-Jacobian			
	0.5	1	2	3	0.5	1	2	3	0.5	1	2	3	0.5	1	2	3
Original	1	4.9	18.1	38.9	1.53	2.78	6.74	11.1	1.49	2.61	6.25	10.24	11.66	19.96	43.88	67.89
Schild's Ladder (BCH)	**1**	**4.85**	**18.8**	**39.5**	1.26	**2.61**	**6.9**	12	**1.29**	2.43	5.71	**9.35**	8.71	16.47	**38.22**	**59.6**
Schild's Ladder (conj)	0.7	2.93	13	29.1	1.3	2.59	6.12	10	1.21	2.41	6.46	11.6	9.6	17.79	37.17	57.72
Conjugate action	.	.	.	.	0.2	1.62	6.11	**11.36**	1.85	**2.54**	4.36	6.57	**13.22**	**18.25**	29.89	43.19
Reorientation	**1**	4.73	17.2	36.5	**1.26**	2.56	6.22	10.7	1.25	2.4	**6.31**	11.6	8.78	16.23	33.9	54.1
Interpolation of scalar maps	0.8	4	14.7	31.4	1.23	2.41	5.94	10	11.9	2.26	5.42	9.1	8.94	16.6	36.2	56.92

Table 2: Average features at the different scaling factors (columns) evaluated in the ventricles mask through the different methods of transport (rows). The L^2 norm of the SVF could not be evaluated with the adjoint method. Bold: closest measure to the original one. The values were multiplied by 100.

Results Figure 4 shows a detail from the median static velocity field from the transported one-year longitudinal trajectories. The field flows outward from the ventricular surface to indicate a pronounced ventricular lateral enlargement. Moreover, we can notice an expansion in the temporal horns of the ventricles as well as a consistent contracting flow in the temporal lobes. The same effect can be statistically quantified by evaluating the areas where the Log-Jacobian maps were statistically different from zero. The areas of significant expansion are located around the ventricles and spread in the CSF areas, while a significant contraction is appreciable in the temporal lobes, hippocampi, parahippocampal gyrus and in the posterior cingulate. We argue that the highly detailed spatial localization of the results underlines the accuracy of the transport.

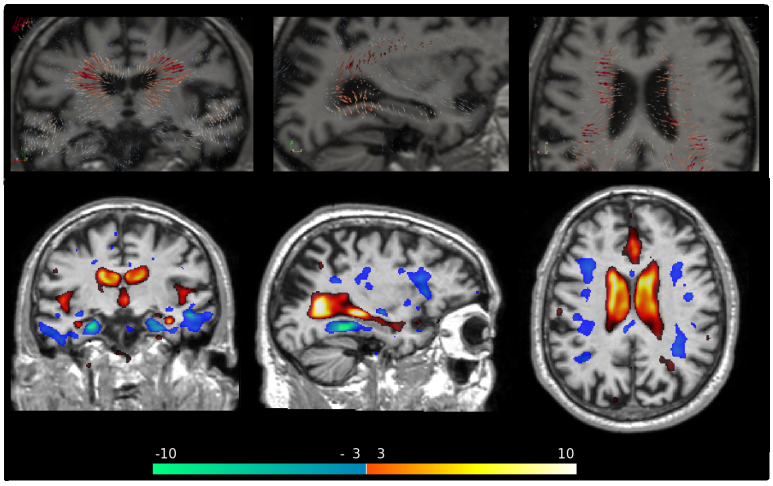

Fig. 4: One year structural changes for 70 Alzheimer's patients. Top row: Median static velocity field. We notice the lateral expansion of the ventricles as well as the contraction in the temporal lobes. Bottom: t-statistic for the areas of Log-Jacobian maps significantly different from 0 ($p < 0.001$ FDR corrected). Blue color: significant contraction, Red color: significant expansions.

4 Discussion and Conclusions

In this study we proposed a novel framework for the transport of longitudinal deformations in a reference space from time series of images. The mathematical formulation was combined with an effective computational scheme in order to provide a reliable and feasible solution for the transport of vector fields. Although designed for transporting vector quantities, the method showed also high accuracy in transporting scalar measures, by preserving smoothness of the

corresponding spatial maps and providing high accuracy on numerical evaluations. This is an interesting feature which could increase the power in TBM-like group-wise statistical analysis as well as opening the way to reliable multivariate groupwise analysis. As a perspective, the association of the Schild's Ladder with specific frameworks for the estimation of longitudinal trajectories [7], will allow to model the progression of changes for specific clinical populations consistently along the temporal dimensions by including multiple time points.

Acknowledgments. This work was partially supported by the French ANR (Agence Nationale de la Recherche) "programme blanc" number ANR-09-BLAN-0332.

References

1. Alexander, D., Pierpaoli, C., Basser, P., Gee, J.: Spatial transformations of diffusion tensor magnetic resonance images. IEEE Transactions on Medical Imaging 20(11) (2001)
2. Bossa, M., M.Hernandez, Olmos, S.: Contributions to 3D diffeomorphic atlas estimation: Application to brain images. MICCAI 10, 667–74 (2007)
3. Bossa, M., Zacur, E., Olmos, S.: On changing coordinate systems for longitudinal tensor-based morphometry. Spatio Temporal Image Analysis Workshop (STIA), MICCAI 2010 (2010)
4. Chung, M., Worsley, K., Paus, T., Cherif, C., Collins, D., Giedd, J., Rapoport, J., Evans, A.: A unified statistical approach to deformation-based morphometry. NeuroImage 14(3), 595–606 (2001)
5. Ehlers, J., Pirani, F., Schild, A.: The geometry of free fall and light propagation, in O'Raifeartaigh. General Relativity, Papers in Honor of J. L. Synge. Oxford University Press (1972)
6. Kheyfets, A., Miller, W., Newton, G.: Schild's ladder parallel transport for an arbitrary connection. International Journal of Theoretical Physics 39(12), 41–56 (2000)
7. Lorenzi, M., Ayache, N., Frisoni, G., Pennec, X.: 4D registration of serials brain's MR images: A robust measure of changes applyed to Alzheimer's disease. Spatio Temporal Image Analysis Workshop (STIA), MICCAI (2010)
8. Miller, M., Trouvé, A., Younes, L.: On the metrics and euler-lagrange equations of computational anatomy. Annu. Rev. Biomed. Rev. 4, 375–405 (2002)
9. Qiu, A., Younes, L., Miller, M., Csernansky, J.: Parallel transport in diffeomorphisms distinguish the time-dependent pattern of hippocampal surface deformation due to healthy aging and dementia of the alzheimer's type. Neuroimage 40(1) (2008)
10. Rao, A., Chandrashekara, R., Sanchez-Hortiz, G., Mohiaddin, R., aljabar, P., Hajnal, J., Puri, B., Rueckert, D.: Spatial trasformation of motion and deformation fields using nonrigid registration. IEEE Transactions on Medical Imaging 23(9) (2004)
11. Vercauteren, T., Pennec, X., Perchant, A., Ayache, N.: Symmetric log-domain diffeomorphic registration: A demons-based approach. MICCAI 5241, 754–761 (2008)
12. Younes, L.: Jacobi fields in groups of diffeomorphisms and applications. Q. Appl. Math (2007)